Products of Endocytosis and Autophagy are Retrieved from Axons by Regulated Retrograde Organelle Transport

Peter J. Hollenbeck

Department of Anatomy and Cellular Biology, Harvard Medical School, Boston, Massachusetts 02115

Abstract. Cellular homeostasis in neurons requires that the synthesis and anterograde axonal transport of protein and membrane be balanced by their degradation and retrograde transport. To address the nature and regulation of retrograde transport in cultured sympathetic neurons, I analyzed the behavior, composition, and ultrastructure of a class of large, phase-dense organelles whose movement has been shown to be influenced by axonal growth (Hollenbeck, P. J., and D. Bray. 1987. *J. Cell Biol.* 105:2827–2835). In actively elongating axons these organelles underwent both anterograde and retrograde movements, giving rise to inefficient net retrograde transport. This could be shifted to more efficient, higher volume retrograde transport by halting axonal outgrowth, or conversely shifted to less efficient retrograde transport with a larger anterograde component by increasing the intracellular cyclic AMP concentration. When neurons were loaded with Texas red–dextran by trituration, autophagy cleared the label from an even distribution throughout the neuronal cytosol to a punctate, presumably lysosomal, distribution in the cell body within 72 h. During this process, 100% of the phase-dense organelles were fluorescent, showing that they contained material sequestered from the cytosol and indicating that they conveyed this material to the cell body. When 29 examples of this class of organelle were identified by light microscopy and then relocated using correlative electron microscopy, they had a relatively constant ultrastructure consisting of a bilamellar or multilamellar boundary membrane and cytoplasmic contents, characteristic of autophagic vacuoles. When neurons took up Lucifer yellow, FITC-dextran, or Texas red–ovalbumin from the medium via endocytosis at the growth cone, 100% of the phase-dense organelles became fluorescent, demonstrating that they also contain products of endocytosis. Furthermore, pulse-chase experiments with fluorescent endocytic tracers confirmed that these organelles are formed in the most distal region of the axon and undergo net retrograde transport. Quantitative ratiometric imaging with endocytosed 8-hydroxypyrene-1,3,6-trisulfonic acid showed that the mean pH of their lumena was 7.05. These results indicate that the endocytic and autophagic pathways merge in the distal axon, resulting in a class of predegradative organelles that undergo regulated transport back to the cell body.

METABOLIC homeostasis in cells requires that the synthesis of macromolecules be balanced by their degradation, and that this balance be regulated so as to allow rapid adaptation to changing conditions. Neurons, and their axonal processes in particular, present a special case for the regulation of homeostasis, since their main synthetic and degradative compartments are located in the cell body, often at a considerable distance from the distal region of the axon. It has long been clear that neurons convey the proteins and organelles synthesized in the cell body outward to the axon via anterograde axonal transport (for review see references 29, 62). However, the means by which the products of degradation are retrieved from the axon to the cell body by retrograde transport are more obscure, as are the putative mechanisms for coordinating the rates of degradation and retrieval with the changing needs of the axon during its growth and maintenance.

Protein degradation is accomplished via both nonlysosomal and lysosomal pathways, the former relying upon diverse cytosolic proteases (13, 25, 33, 55), and the latter relying upon the process of autophagy, by which cytoplasmic contents are either nonspecifically sequestered within a boundary membrane and delivered by fusion to the lysosomal compartment (37, 40, 69), or specifically translocated across the lysosomal membrane (14). Degradation via the nonspecific autophagic-lysosomal pathway can be stimulated to increase by stress, nutrient deprivation, and hormone stimulation, allowing the cell to adjust the rate of degradation to its current conditions (49, 66). Experimental manipulations have demonstrated two significant control points in the pathway: the initial sequestration of cytosolic proteins into autophagic

Dr. P. Hollenbeck's current address is Department of Neurobiology, Harvard Medical School, 220 Longwood Avenue, Boston, MA 02115.

vacuoles (26, 41, 54, 63, 67), and autophagic vacuole fusion with lysosomes (38, 68). A level of regulation intermediate to these two—that of the transport of autophagic vacuoles from their sites of formation to the lysosomes—has received less attention. Although the disruption of microtubules has been shown in several cell types to inhibit autophagosome-lysosome fusion (e.g., 42, 58, but cf. 56, 57), these studies have generally been interpreted in the light of the notion that microtubule-based motility facilitates but is not essential for organelle movements over short distances in nonneuronal cells.

In neurons, however, it is clear that microtubule-based transport is critically important to convey organelles along the axon (2, 29, 61, 62). Since the growth cone or synapse is separated from the main lysosomal compartment by the length of the axon, the formation of autophagic vacuoles is separated from their fusion with the lysosomes by a much larger distance, and presumably a longer time, than in nonneuronal cells. Thus, it seems likely that the nature and regulation of retrograde axonal organelle transport are central to the regulation of the autophagic-lysosomal pathway of protein degradation in neurons.

In this study, I have examined the role of retrograde transport in cellular homeostasis using embryonic peripheral neurons grown in culture. When these cells are viewed by phase contrast microscopy, the most prominent organelles seen are large, ovoid, refractile structures that undergo transport in both the anterograde and retrograde directions (35). Their abundance and the fraction of them moving retrogradely have previously been demonstrated to increase when axonal outgrowth is blocked. Since this is a condition in which the quantity of protein and membrane being delivered to the axonal tip by slow and fast anterograde axonal transport is expected to exceed the amount required to construct new axon, it was proposed that these organelles could serve to retrieve protein and membrane from the distal region of the axon (35). Here I report that these organelles show a highly plastic transport behavior in which the efficiency and volume of their retrograde transport is modulated by the physiological state of the neuron, and demonstrate that they contain material derived both from endocytic uptake and from bulk sequestration of cytoplasm. Thus, they link the lysosomal compartment in the cell body with autophagic and endocytic events of the distal axon, providing a regulated retrograde flux that balances anterograde axonal transport.

Materials and Methods

Materials

All reagents, culture media, and supplements were obtained from Sigma Chem. Co. (St. Louis, MO) unless otherwise specified. Lucifer yellow, Texas red–conjugated ovalbumin, 8-hydroxypyrene-1,3,6-trisulfonic acid, and fluorescent dextrans were obtained from Molecular Probes (Eugene, OR). Formaldehyde, glutaraldehyde, OsO_4, and Epon were obtained from Electron Microscopy Sciences (Fort Washington, PA). Forskolin was stored as a 20-mM stock in 100% ethanol at 4°C. Cytochalasin E was stored frozen as a 2-mg/ml stock in 100% DMSO.

Cell Culture

Sympathetic ganglia from E9-E10 chick embryos were dissected into HBSS and dissociated by incubation for 20 min at 37°C in Ca^{2+}- and Mg^{2+}-free HBSS containing 0.25% trypsin. They were then washed with complete HBSS, dissociated into individual neurons by trituration in HBSS, and diluted to ~100 cells/ml in Leibowitz L-15 medium supplemented with 10% FBS, 0.6% glucose, 2 mM L-glutamine, 100 U/ml penicillin, 100 μg/ml streptomycin, 0.5% methylcellulose (Dow Chemical Co., Indianapolis, IN), and 50 ng/ml 2.5S mouse nerve growth factor (Boehringer Mannheim, Indianapolis, IN). Aliquots of this suspension were placed either into the wells of 6-well plates containing 22 × 22 mm glass coverslips (for light microscopy) or into a 60-mm culture dish with a 25 × 25-mm coverslip mounted over an 18-mm hole drilled in the bottom of the dish (for correlative light and electron microscopy), as previously described (35). Before use, coverslips were washed with alcohol, dry sterilized, and treated in succession with 1 mg/ml poly-L-lysine, and a laminin-enriched fraction of conditioned medium (44). For observation of neurons at short times after plating, cells were deposited onto the substratum by gentle centrifugation rather than passive settling. Cells were grown in a humidified 37°C incubator for 12-48 h before observations.

Light Microscopy

Coverslips containing neurons were mounted upside down on a 24 × 60-mm glass coverslip using coverslip fragments as spacers, and the chamber was sealed with a 1:1:1 mixture of vaseline, lanolin, and paraffin. Chambers were mounted on the 37°C heated stage of a IM35 microscope (Carl Zeiss, Inc., Thornwood, NY), and observed using phase contrast and/or epifluorescence optics with a 63× Planapochromatic objective and an oil immersion condenser. For correlative light and electron microscopy and ratiometric imaging, cells were observed on coverslips mounted on the bottom of drilled out culture dishes using a long working distance condenser. Photomicrographs were taken using Kodak TMAX 100, 400, or 3200 film. Video records were made using a Hamamatsu C2400 newvicon camera, an Image-1 image processor (Universal Imaging Corp., West Chester, PA), and a Panasonic AG7300 sVHS recorder. Organelle movements were tracked from sVHS video recordings with a microcomputer-based system consisting of a Mark IV video board (Michael Walsh Electronics, Pasadena, CA) and Measure software (provided by Dr. S. M. Block).

Drug Treatments and Control of Outgrowth

Before treatment with drugs or uptake markers, cultures were transferred to medium without methylcellulose to reduce viscosity and promote mixing. Forskolin (25–200 μM), cholera toxin (0.3–2.4 μM), or 8-Br-cAMP (1–2 mM) were made up in culture medium into which coverslips were transferred for 20 min before the observation and quantification of organelle movements for 40 min. Axonal outgrowth was halted by one of two methods, as previously described (35). Briefly, neurons were (*a*) plated onto coverslips which had first been siliconized and then shadowed with SiO through a metal foil stencil to create 7-μm-wide hydrophilic strips 50–800 μm long to which cell adhesion and growth were limited. Growth cones arriving at the end of a strip halted and became inactive. (*b*) Neurons were grown on laminin-treated coverslips as described above; then the cultures were treated with 1 μg/ml of cytochalasin E, which stopped protrusive activity and growth cone advance but did not cause axonal retraction during the period of observation.

Endocytic and Cytosolic Labeling of Live Cells

To fluorescently label endosomes and pinosomes, 500 μg/ml Lucifer yellow (LY)[1], 100 μg/ml Texas red–conjugated ovalbumin (TR-Ov), 400 μg/ml 10 kD fluorescein isothiocyanate–conjugated dextran (FITC-Dx), or 1 mM 8-hydroxypyrene-1,3,6-trisulfonic acid (HPTS) were added to culture medium for 1–18 h and washed out before observation. For fluorescent labeling of cytosol, neurons were loaded by trituration (11) of trypsinized ganglia in 5 mg/ml of 10 kD TR-Dx, and then the cell suspension was diluted 1,000-fold with medium, and cells were plated out on coverslips as usual. After 4–8 h of growth, the cultures were washed thoroughly with HBSS and placed in fresh medium. As a control for the potential endocytic labeling of organelles by uptake of residual TR-Dx left in the medium after trituration-loading, separate ganglia were triturated in the absence of fluorescent label, and the dissociated neurons were then grown for 4–8 h in medium containing the same concentration of TR-Dx that was present

1. *Abbreviations used in this paper*: HPTS, 8-hydroxypyrene-1,3,6-trisulfonic acid; LY, Lucifer yellow; FITC-Dx, fluorescein isothiocyanate-conjugated dextran; TR-Ov, Texas-red-conjugated ovalbumin.

in the trituration-loaded cultures after dilution with medium. For double labeling of cytosol and endosomes/pinosomes, neurons were triturated in TR-Dx as described above, grown 24–48 h, and were then transferred to medium containing 400 μg/ml of FITC-Dx.

Determination of pH

Acridine orange (5 μg/ml) was added to culture medium for 15–30 min with or without 10 mM NH_4Cl, washed out, and cells were observed and photographed using epifluorescent illumination with a standard Texas red filter set. For quantitative pH determination, phase-dense organelles were labeled by endocytic uptake of 1 mM HPTS (12, 24, 79) from the medium for ≥1 h. Cultures were then washed with unlabeled medium and viewed by phase contrast and epifluorescence optics with a fluorescein filter set. Excitation light was provided by a Tracor Northern Fluoroplex system (Noran Instrs. Inc., Middleton, WI), with alternating 405 and 450 nm wavelength light transmitted through a pair of intermeshed optical fiber cables. Fluorescent images were gathered with a newvicon video camera equipped with a multichannel plate image intensifier (Videoscope International, Washington, DC), and the signal was processed with a Tracor Northern TN8500 image processing system, recording digital images after Kalman averaging of 50 video frames. After identifying phase-dense organelles using phase contrast optics, fluorescent images were gathered by using a light chopper to alternately average 10 video frames at each wavelength five times in rapid succession. Background images were collected in the same manner from an adjacent region of the coverslip, and subtracted digitally from the stored images. The 450-nm image was then divided by the 405-nm image to obtain a ratio image, and the mean fluorescence ratio of each organelle was determined using a binary mask that restricted calculation to the pixels occupied by the organelle image. To establish an in situ standard curve for the relationship between fluorescence ratio and pH, neuronal cultures loaded with HPTS were incubated with 10 μg/ml nigericin in 130 mM KCl, 15 mM Hepes, 15 mM MES buffer over a pH range of 5.0–7.6, and the fluorescence ratios of 10–20 organelles from several neurons were determined at each pH.

Correlative Light and Electron Microscopy

Light microscope video records were made of phase-dense organelles moving in regions with distinctive arrangements of axons, then while continuing the recording, the cultures were fixed by addition to the medium of a large volume of 0.3% formaldehyde, 0.625% glutaraldehyde, and 0.0075% picric acid in warm unsupplemented L-15 medium. After 10 min, cultures were transferred to fresh fixative for 10 min, and were then processed and embedded as follows: pH 7.2 cacodylate buffer wash, 30 min incubation in cacodylate buffer containing 1% OsO_4, cacodylate buffer wash, pH 5.2 maleate buffer wash, 30 min in maleate buffer containing 1% uranyl acetate, maleate buffer wash. Processed cultures were then dehydrated and embedded in a wafer of Epon. The coverslips were then dissolved off of the plastic wafers by HF treatment, and the original field of view was relocated by light microscopy using the video record as a guide. A small blockface containing the original field was cut from the plastic wafer and thin-sectioned in the plane of the original culture substratum. Sections were picked up on formvar-coated slot grids and stained briefly with saturated uranyl acetate followed by lead citrate. Sections were viewed using a JEOL 100CX electron microscope and the original microscopic field was located and photographed at low and high magnification.

Results

Regulation of Organelle Motility

In contrast to the smooth unidirectional movements of organelles seen in invertebrate giant axons (1) and in reactivated in vitro axonal transport models (4, 78) the phase-dense organelles in sympathetic neurons underwent saltatory movement as they traversed the axon, with frequent stops and changes of direction (Fig. 1). Although they underwent net

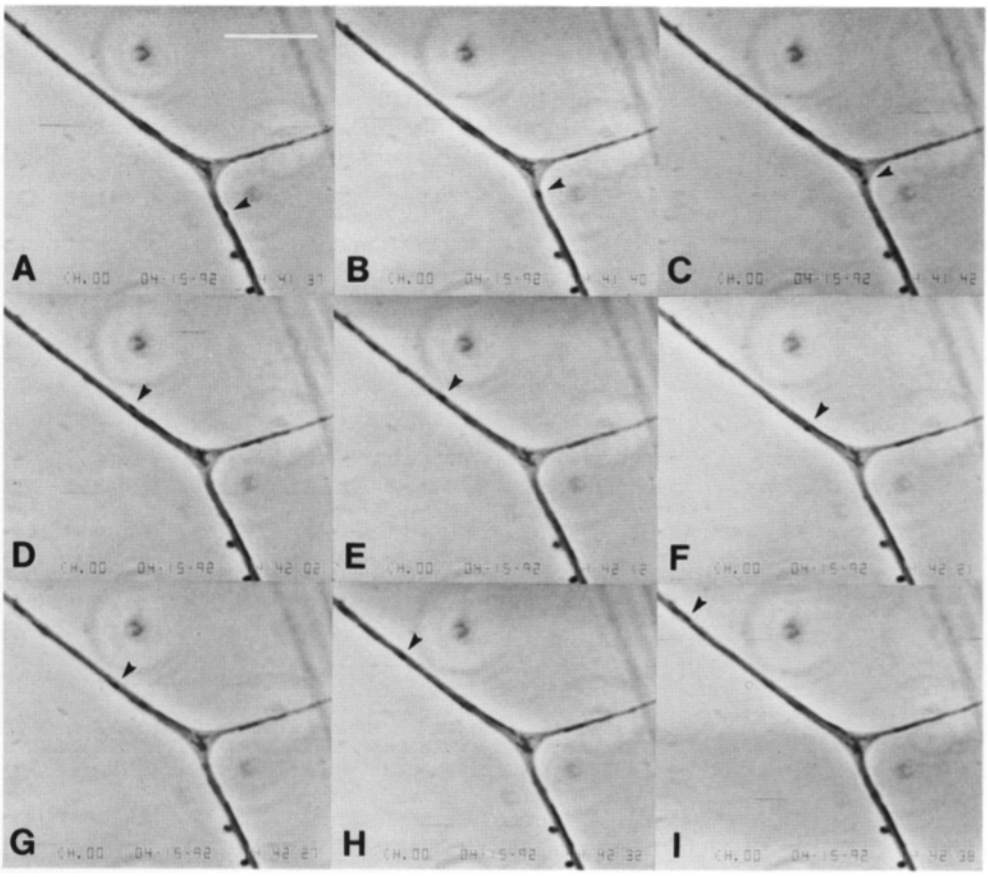

Figure 1. The movement of a phase-dense organelle along a branched axon, shown by video-enhanced phase contrast microscopy. The cell body is far out of the field to the upper left, and the growth cones of the two branches are out of the field to the bottom and right. A phase-dense organelle (*arrowheads*) moves retrogradely into the branch point (*A–C*), and back onto the main axon (*D*), slows down (*E*), and reverses direction, moving 6 μm anterogradely (*F*). After a short pause, it again reverses direction, moving retrogradely (*G–I*). The time course of the sequence is indicated by the digital display at the lower right of each video field. Bar, 10 μm.

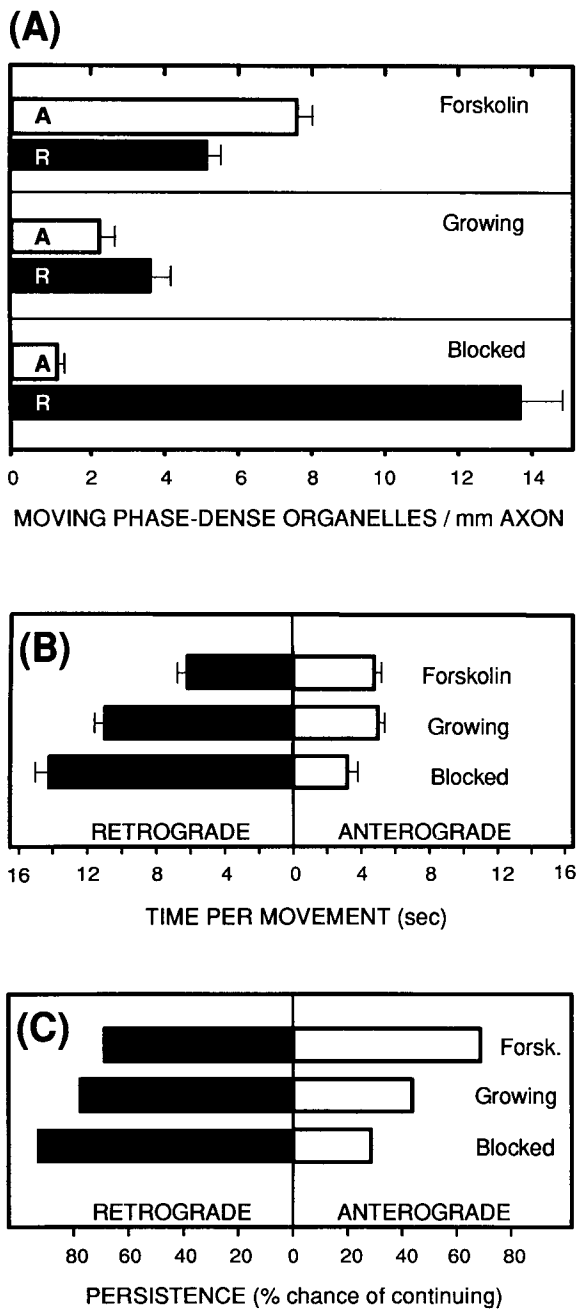

Figure 2. Experimental manipulation of the direction of transport of phase-dense organelles. (*A*) Instantaneous measurements of the number of phase-dense organelles moving in each direction per mm of axon under three different growth conditions: forskolin-containing medium, normal medium (*growing*), and cytochalasin-containing medium (*blocked*). Anterograde bars are marked *A*, retrograde bars, *R*. Each bar represents the analysis of the movement of 96–236 organelles on 61–72 neurons in 3–5 separate experiments. Error brackets indicate 1 SEM. (*B*) The mean duration of movement between stops is shown for the anterograde and retrograde directions under all three growth conditions. Each bar represents analysis of the behavior of 25–227 separate organelle movements on 24–40 axons. Error brackets indicate 1 SEM. The mean for retrograde movements in both forskolin-treated and blocked axons, and for anterograde movements in blocked axons, differed significantly from those in growing axons ($P < 0.01$ in a two-sample, one-tailed *t* test). (*C*) The % chance of an organelle continuing in its original direction of movement after a stop is shown for all three conditions. Each bar represents pooled percentage data from 48–116 organelle movements on 24–40 axons analyzed under each condition, over a total of ~100 organelle-min of observation.

retrograde transport in growing axons, this could be biased more highly in the retrograde direction by halting axonal elongation using substratum-associated barriers or drug treatment (35). To analyze the regulation of transport in more detail, conditions were sought that would produce the opposite effect: biasing their movement in the anterograde direction. Three different agents that increase intracellular cAMP in neurons—forskolin (64, 65), cholera toxin (7, 8, 23, 47), and 8-Br-cAMP (20)—each gave a dose-dependent increase in the ratio of anterogradely moving/retrogradely moving phase-dense organelles. For the following analyses of the regulation of organelle behavior, forskolin, whose effect on transport plateaued at 100 μM, was used to promote anterograde movement.

As a simple measure of the net flux of organelles under the three different growth conditions, instantaneous measurements of the number of phase-dense organelles moving in each direction per mm of axon were made (Fig. 2 *A*). The ratio of retrogradely/anterogradely moving organelles was 1.6 in growing axons and this fell to 0.6 in forskolin-treated axons, and rose to 11.2 in axons with their outgrowth blocked. In addition, the mean number of total phase-dense organelles present per mm of axon rose from 6.2 (SEM = 1.1, $n = 96$) in growing axons, to 8.1 (SEM = 0.8, $n = 81$) in forskolin-treated axons, and further to 14.9 (SEM = 1.8, $n = 258$) in blocked axons. To determine what specific aspects of transport behavior were altered under conditions that biased the retrograde/anterograde ratio, the mean duration of anterograde and retrograde movements between stops were determined for all three growth conditions (Fig. 2 *B*). The mean retrograde and anterograde movements were 11s and 5s, respectively, in growing axons. Forskolin treatment decreased the duration of the average retrograde movement relative to untreated controls without affecting the duration of anterograde movements. Blocking axonal outgrowth increased the duration of retrograde movements and decreased that of anterograde movements. The regulation of direction switching was analyzed by determining under all three conditions the probability that an organelle would continue in its original direction of movement after a stop. Forskolin treatment increased the probability of persistent anterograde movement and decreased the probability of persistent retrograde movement relative to control cultures, while blocking axonal outgrowth had the opposite effect (Fig. 2 *C*).

Autophagic Tracers

Previous immunocytochemical evidence has suggested the phase-dense organelles contain cytosolic proteins (35), presumed to be enclosed in membrane by autophagy. To assess whether this might be the case, the cytosol of neurons was loaded with 10 kD TR-Dx, an inert fluorescent marker that is sequestered by autophagy and delivered to the lysosomal compartment, but not degraded (31). Triturating the ganglia in TR-Dx during the standard dissociation introduced the label into virtually 100% of the cells by transient membrane wounding (11); they were then plated out and grown as usual.

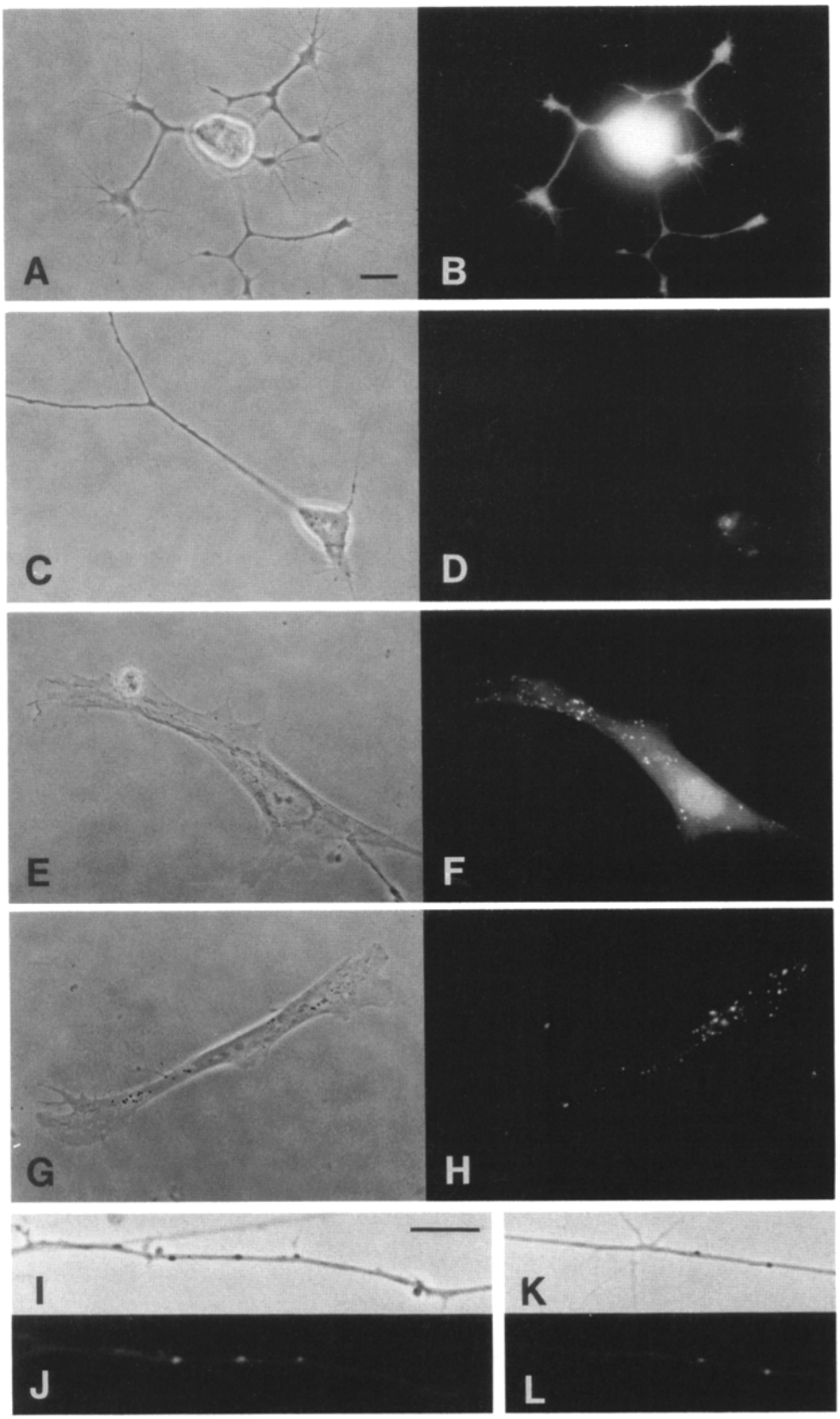

Figure 3. Sequestration of cytosolic TR-Dx into phase-dense organelles. Live cells are shown in phase contrast (*A*, *C*, *E*, *G*, *I*, and *K*) and paired epifluorescence (*B*, *D*, *F*, *H*, *J*, and *L*) micrographs. Several hours after cytosolic loading with TR-Dx, neurons showed uniform diffuse staining (*A* and *B*); fibroblasts showed diffuse staining and already displayed some punctate staining (*E* and *F*). Over 48 h in neurons, and a shorter period in fibroblasts, the general cytosolic staining disappeared, and the distribution of label became entirely punctate (neuron: *C* and *D*, fibroblast: *G* and *H*). During this time, the phase-dense organelles in axons became intensely fluorescent (*I–L*, note higher magnification). Bars, 10 μm.

As previously described for fluorescent proteins injected into nonneuronal cells (71), TR-Dx initially labeled the neuronal cytoplasm uniformly and intensely (Fig. 3, *A* and *B*), but over a period of 48 h, the label was cleared from the cytosol of axons and ended up in a punctate, presumably lysosomal, compartment near the nucleus (Fig. 3, *C* and *D*). The sequestration process is more easily seen for the entire cell by viewing the nonneuronal cells present in sympathetic

ganglion cultures (Fig. 3, *E–H*). In neurons, during the period in which the label was being cleared from the axons to the cell bodies, 100% of the phase-dense organelles were brightly fluorescent (Fig. 3, *I–L*), and they were the major fluorescent structure in the axon. These data indicate that the phase-dense organelles sequester cytoplasmic contents.

Control experiments were performed to rule out two possible alternative explanations of these results. The first was that the apparent autophagic sequestration of cytoplasmic label by phase-dense organelles could actually have resulted from endocytic uptake of residual TR-Dx left in the medium after trituration loading and dilution of the cells. To address this, cultures were triturated in the absence of label, and then grown for several hours in the concentration of TR-Dx that would have remained in the medium after trituration loading and dilution (~5 μg/ml); this treatment did not result in fluorescent labeling of phase-dense organelles. A second possibility was that the slow sequestration of TR-Dx resulted not from autophagy, but from slow cleavage of Texas red from the dextran molecule, superimposed upon rapid sequestration of the free dye via nonautophagic mechanisms such as organelle membrane ion transport (72). Although the absence of any known zwitterionic organelle membrane pump made this unlikely, we addressed the possibility by trituration-loading neurons with unconjugated Texas red at molar concentrations ≥ the concentration that had been delivered as dextran-conjugated dye. These cells sequestered cytosolic fluorescent label with the same time course as the TR-Dx–loaded cells, clearing the label slowly from a diffuse cytosolic distribution to an exclusively punctate one in 48–72 h, and thus indicating that there was no rapid sequestration mechanism delivering free dye into the phase-dense organelles (not shown).

Organelle Ultrastructure

To extend the analysis of this class of organelles—previously defined only by its appearance and behavior at the light microscope level—to the ultrastructural level, correlative light and electron microscopy were performed. Video recordings of axons containing moving phase-dense organelles were made using phase contrast optics, and then the cultures were fixed, processed, and embedded for transmission electron microscopy. Video records were used to identify the original light microscope fields in thin sections cut parallel to the original culture substratum, and 29 phase-dense organelles of known behavior and appearance before fixation were relocated from 11 different light microscope fields. The ultrastructure was relatively consistent among organelles: each had a bilamellar or multilamellar boundary membrane of varying thickness, and a granular lumen that contained variably recognizable cytoplasmic contents such as vesicles

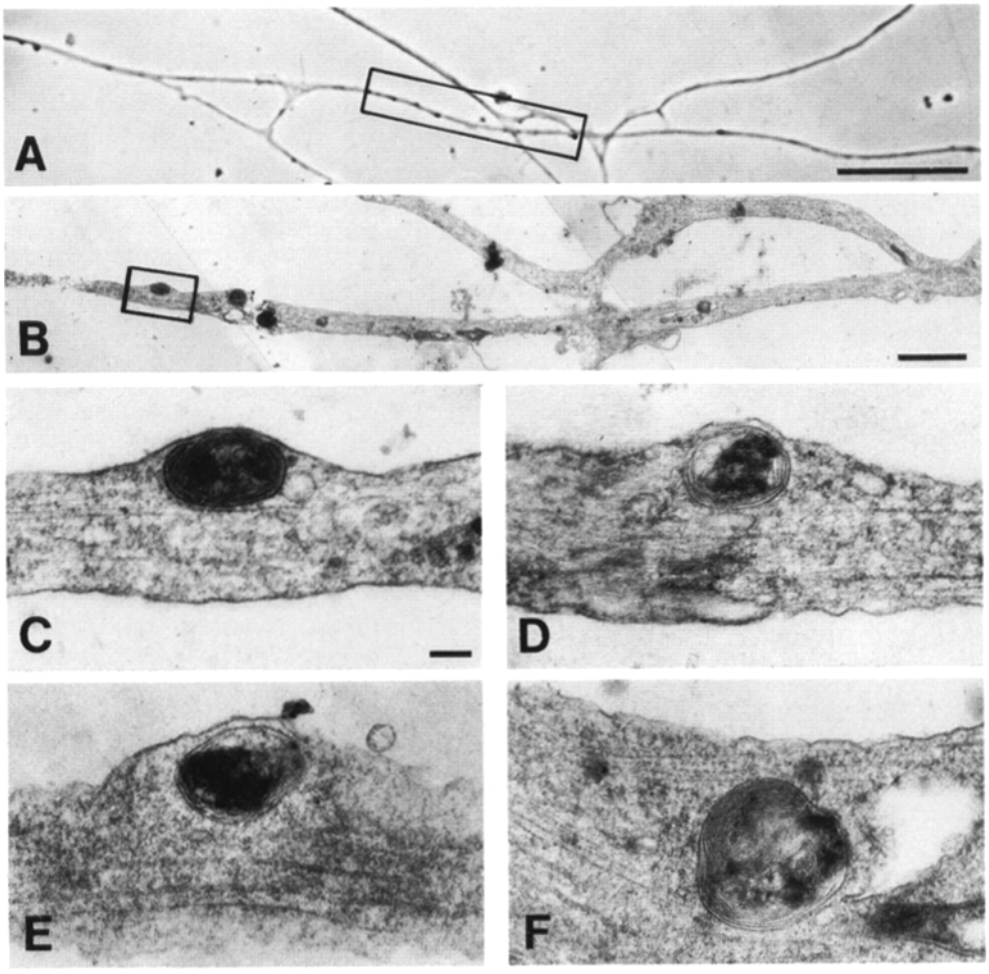

Figure 4. Correlative light and electron microscopy. Moving phase-dense organelles were observed by phase contrast microscopy and recorded on video tape and 35 mm negatives before fixation. *A* is a light micrograph taken at the time of fixation. The boxed area contains three phase-dense organelles that were moving at the time of fixation. Bar, 20 μm. *B* is a low magnification thin section electron micrograph of the region outlined by a black box in *A*. The organelles had moved slightly between the time that *A* was taken and the moment of effective fixation. Bar, 2 μm. *C* shows the region outlined in *B* at higher magnification, demonstrating the fine structure of one of the moving organelles. Bar, 0.2 μm. *D*, *E*, and *F* show other examples of phase-dense organelles that were first identified at the light microscope level and then relocated in thin sections; these were chosen to represent the range of variation in morphology that was seen. During the period of observation before fixation, these organelles moved retrogradely (*E*), anterogradely (*D*), or in both directions (*C* and *F*).

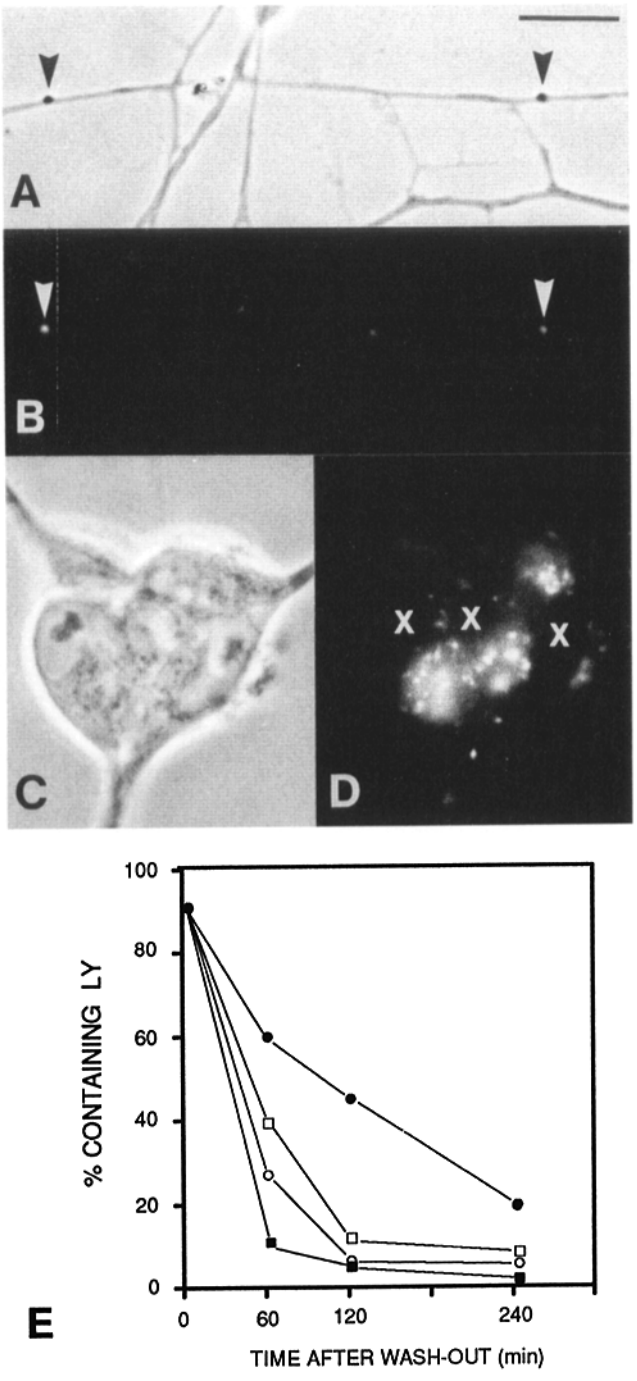

Figure 5. Lucifer yellow uptake into phase-dense organelles. When neurons were allowed to take up lucifer yellow or other markers from the culture medium by endocytosis, the phase-dense organelles (*A, arrowheads*) became brightly labeled (*B*, same field viewed by epifluorescence). After washing lucifer yellow out of the culture medium for 4–16 h, punctate fluorescence accumulated in the cell bodies; here a cluster of three cell bodies is shown in phase contrast (*C*), with the areas of the nuclei, which excluded label, indicated by x's in a paired fluorescence micrograph (*D*). Bar, 10 μm. After fluorescent label was washed out of the culture medium, the percent of phase-dense organelles that were fluorescent was quantified (*E*) at time intervals up to 240 min for the entire axon (●) and for three adjacent axonal segments: the most distal 100 μm of axon (immediately proximal to the growth cone) (■); the 100 μm segment between 100 and 200 μm from the growth cone (○); and the 100 μm segment between 200 and 300 μm from the growth cone (□). The four descending curves demonstrate that lucifer yellow was cleared fastest from the most distal region of the axon, and exited the axon vectorially, from distal to proximal regions, toward the cell body. The departure from 100% of the initial time point on the curves is an artifact of the chasing of fluorescence that occurred during the time necessary to make the initial measurements. Each point on each curve represents 40–120 organelles scored on 20–26 separate axons.

(Fig. 4). This is in general similar to predegradative autophagic vacuoles as described in these neurons (6) and in nonneuronal cells (e.g., 16). Their appearance did not vary in any systematic way with the direction that the organelle was moving before fixation.

Endocytic Tracers

The autophagic tracer experiments described above indicated that phase-dense organelles convey sequestered cytoplasm, but since they appeared to undergo net retrograde transport, it seemed possible that they were also conveying products of endocytosis away from the growth cone. To test this, active growth cones were allowed to take up LY, TR-Ov, or FITC-Dx from the culture medium by endocytosis. Under these conditions, 100% of the phase-dense organelles became brightly fluorescent (n = 244), and they were the most prominent fluorescent structures in the axons (Fig. 5, *A* and *B*), although small fluorescent structures, presumably conventional endosomes or multivesicular bodies (51), were also apparent (see Fig. 6, *A* and *B*). When fluorescent label was removed from the medium, it was chased back to the cell bodies where it assumed a punctate juxtanuclear distribution (Fig. 5, *C* and *D*). To confirm quantitatively that the endocytosed material was undergoing net retrograde transport in these organelles, a pulse-chase experiment was performed: 48-h-old neuronal cultures with axons ~1,000 μm in length were incubated with LY-containing culture medium for 12–18 h, and then the labeled medium was replaced with normal medium, and the % of phase-dense organelles that were fluorescent was quantified at time intervals for different regions of the axon. Over a 4-h chase period, the % of phase-dense organelles that were fluorescent along the entire axon dropped steadily (Fig. 5 *E*) and the fluorescence accumulated in the cell body. More important, fluorescent organelles were cleared most quickly from the 100-μm segment of each axon nearest the growth cone, followed by more proximal segments in order of their distance from the growth cone (Fig. 5 *E*). Thus, after the removal of endocytic tracer from the medium, a wave of unlabeled organelles swept retrogradely down the axons from their tips. These data demonstrate that the phase-dense organelles support a vectorial traffic of endocytic label from the growth cone to the cell body. Anterograde axonal transport of fluorescent organelles derived from endocytosis at the cell body was not observed.

The 100% labeling of phase-dense organelles via both autophagic and endocytic tracers indicated that products of endocytosis and autophagy were indeed being targeted to the same individual organelles, but to confirm this, neurons were double-labeled by introducing TR-Dx into the cytosol by trituration-loading, grown for 24 h, and then endocytically labeled by uptake of FITC-Dx from the medium. These

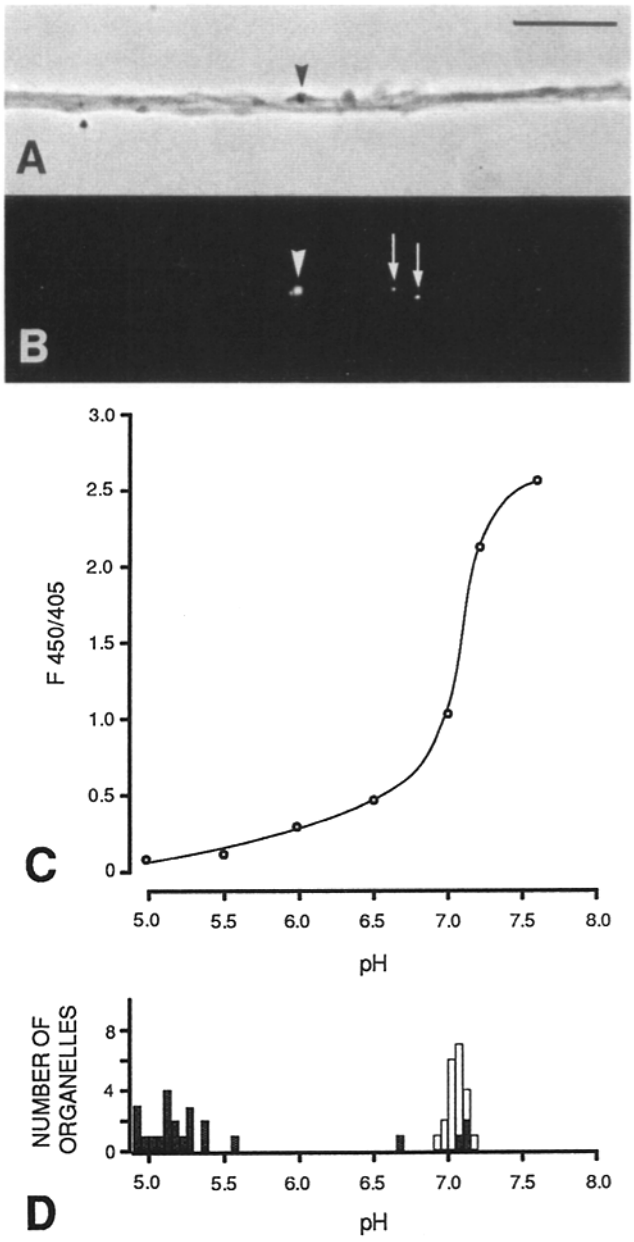

Figure 6. pH of phase-dense organelles. Phase contrast microscopy (*A*) and epifluorescence microscopy (*B*) of a live neuron allowed to take up HPTS from the culture medium shows the bright fluorescence of the large phase-dense organelle (*arrowhead* in both micrographs) in addition to the smaller conventional endosomes or multivesicular bodies that are invisible in phase (*arrows* in *B*). Bar, 10 μm. (*C*) Quantitative pH determination. The standard curve for clamped organelle pH vs. the ratio of fluorescence intensities at 450 and 405 nm excitation shows the high sensitivity of the fluorescence ratio to pH in the physiological range. Each point is the mean of the ratio for 10–20 organelles in several different neurons. (*D*) The distribution of pH values determined for phase-dense organelles in axons (*clear bars*) and various organelles in cell bodies (*shaded bars*). Some organelles in the cell bodies (4/28) had fluorescence ratios lower than the lowest point on the standard curve and were not included here. Data are derived from 11 axons and 10 cell bodies.

experiments confirmed the results of separate experiments with endocytic and cytoplasmic tracers: the phase-dense organelles were positive for both labels, and thus contained material from both pathways (not shown).

pH Determination

To determine whether the phase-dense organelles were acidic, cultures were incubated briefly with the fluorescent weak base acridine orange. This resulted in the phase-dense organelles becoming brightly fluorescent; however, simultaneous treatment of cultures with the competing weak base ammonium ion failed to eliminate acridine orange fluorescence in the phase-dense organelles, indicating that acridine orange was not an accurate reporter of lumenal pH for these organelles. This prompted quantitative pH determination. In these experiments, neurons were allowed to take up HPTS by endocytosis from the culture medium (Fig. 6, *A* and *B*), and the phase-dense organelles were analyzed in live cells by ratiometric imaging (24). Endocytically labeled neurons were also used to prepare a pH standard curve for organelles in situ using standard pH buffers and the ionophore nigericin. This established for organelles the sensitivity of HPTS fluorescence to pH variation in the physiological range (Fig. 6 *C*), as has been reported for phospholipid and flagellar membrane vesicles in vitro (12, 39, 45), and for cytosol (21, 22, 24, 48). Measurements on phase-dense organelles taken throughout the axons gave a mean pH value of 7.05 (SD = 0.06, n = 21). Few if any endocytically labeled axonal organelles of any kind were acidic, although the pH organelles in the cell body routinely ranged from <5 to 7 (Fig. 6 *D*).

Discussion

During neural development, anterograde axonal transport delivers to the region of the active growth cone the protein and membrane necessary for the construction of new axon. When axonal outgrowth slows or halts temporarily during development, or when it stops completely upon the formation of a synapse, the anterograde flow continues, raising the question of how the distal axon achieves material homeostasis. Retrograde organelle transport is well known to convey important products of endocytosis from the terminal to the cell body (e.g., 15, 18, 32, 43), and radiolabeling studies have indicated that it also retrieves endogenous macromolecules (29). However, despite the identification via axonal disruption studies of various putative predegradative structures as part of the retrograde flow (e.g., 19, 70, 74), the properties of that traffic and its relation to other events in the distal axon has remained unclear. We have previously shown that in peripheral neurons, one class of retrogradely moving organelles increases in number and displays more efficient net transport under conditions designed to maximize the excess of material arriving at the axonal tip (35). We proposed that this particular class of organelles might serve to balance anterograde transport with the varying needs of the distal axon by retrieving an appropriate amount of excess cytoplasmic material back to the cell body. Here I have addressed this hypothesis by analyzing the behavior, properties, and ultrastructure of these organelles.

Properties and Ultrastructure

The properties of the phase-dense organelles are consistent with a bulk retrieval function. Their bright fluorescence during autophagic clearing of fluorescent dextran from axoplasm showed that they sequester cytoplasmic contents, and their net retrograde transport indicates that they must arise in the distal axon and convey their contents to the cell body. In addition, correlative electron microscopy revealed that

their ultrastructure is similar to that of early autophagic vacuoles (e.g., 16, 17), bearing in mind the considerable variation in morphology of autophagic vacuoles seen in these neurons (6). They could bear some relation to the multivesicular bodies seen in the distal axon, which are accessible to exogenous tracers (5, 36, 51). However, this is unlikely since these seem not to persist throughout retrograde transport (5), and in this study of peripheral axons, images of multivesicular bodies were rare. They are unlikely to be degradative, since they are not acidic (Fig. 6), and since maturation of autophagic vacuoles from the early to the degradative stage is thought to be accompanied by reduction of the multilamellar membrane to a single one (16, 63). It also requires fusion of the vacuoles with lysosomes or dense bodies, an event which seems unlikely because of the paucity of these elements in the distal axon (53). In addition, the phase-dense organelles did not stain positively for acid phosphatase or mannose-6-phosphatase receptor (not shown). These data, taken together with previous evidence that they contain cytoskeletal proteins and membrane (35), indicate that these organelles are neuronal predegradative autophagic vacuoles.

The origin of the vacuolar membrane in axons is likely to differ from that of autophagic vacuoles in nonneuronal cells. In hepatocytes, for instance, it is clear that cytoplasm is sequestered into autophagic vacuoles by membrane derived from denuded areas of the rough ER (16). Here however, the organelles are arising in the distal axon, an area devoid of bona fide rough ER. Nonetheless, the organelle-rich region of the growth cone has other potential sources of membrane for autophagic vacuole formation, including elements of smooth ER (53) as well as the membranous tubules or cisternae found near the terminal (e.g., 9, 30, 34, 36, 46, 59). The latter structures appear to be involved in local recycling in the growth cone, since they receive products of endocytosis by fusion and may also supply membrane for exocytosis (10). If such an intermediate recycling compartment, whose lumen contains products of endocytosis, also supplies membrane for autophagic vacuole formation it would explain another result seen in this study: the presence in the neuronal vacuoles of fluorescent tracer derived not only from cytoplasm, but also from endocytosis in the growth cone region (not shown). A class of organelles that constitutes a prelysosomal fusion of the endocytic and autophagic compartments has been described in hepatocytes by Gordon et al. (27, 28), who designated it the amphisome. In the axon, the occurrence of both endocytosis and autophagic vacuole formation in the region of the growth cone, along with the potential differences in autophagic vacuole formation discussed above, may make such a dual compartment more likely to occur than in nonneuronal cells. In addition, the long retrograde transit that intervenes between its formation and delivery to the lysosome increases its residence time in the neuron, making it a more prominent organelle in axons.

Significance of Regulated Organelle Motility

Although axonal autophagic vacuoles underwent net retrograde transport, they made both anterograde and retrograde movements, and in actively elongating axons their retrograde progress was relatively inefficient. Conditions that halt axonal outgrowth reduced the fraction of time that they spent moving in the anterograde direction and increased the fraction spent moving in the retrograde direction, while treatments that elevate intracellular cAMP had the opposite effect. Both effects were due to direction-specific changes in the length and persistence of movements (Fig. 2), indicating specific regulation of motility. Thus, axonal autophagic vacuoles provide a clear example of highly plastic organelle motility that is regulated in concert with physiological conditions. But why should the movement of retrogradely transported structures contain an anterograde component? As a consequence of being composed of membrane that was originally delivered to the distal axon by anterograde transport, these organelles probably bear functional anterograde motor proteins (3, 74–77) or their receptors (73; Toyoshima, I., J. Lockman, H. Yu, and M. P. Sheetz. 1991. *J. Cell Biol.* 115:381*a*.) on their surfaces, in addition to retrograde motors (52, 60). Although the continued activity of the anterograde motors could be merely a kind of statistical "noise," its modulation by changes in physiological conditions (Fig. 2) argues that it is more likely to be specifically regulated in concert with retrograde movements.

This raises the larger question of why autophagic vacuole transport should be regulated at all. In nonneuronal cells, the rate-limiting step in autophagy is the initial sequestration of cytoplasm into vacuoles (50), and evidence suggests that this is the major control point in the pathway (26, 41, 54, 63, 67). It is clear from the analysis performed here of organelle numbers and movements that autophagic vacuole formation is highly regulated in neurons as well: although the more efficient retrograde movement induced by halting outgrowth must clear organelles out of the axon more rapidly, the number of organelles per unit length of axon under these conditions actually increased 2.4-fold, indicating an even larger increase in their rate of formation in the distal axon (Fig. 2). But because of the functional asymmetry of the neuron, autophagy must not only sequester cytoplasm, but must also redistribute it regionally. The regulation of motility revealed in this study accomplishes this, matching the increased rate of organelle formation under conditions of blocked outgrowth with a modulation of transport behavior that retrieves them to the lysosomal compartment in the cell body more quickly and also presumably yields a regulation of axonal volume that is appropriate to the growth conditions of the neuron. An additional possibility is that the rate of transport along the axon influences their degree of acidification and likelihood of fusion with hydrolase-bearing vesicles in the vicinity of the cell body, both of which could affect the overall rate of autophagic degradation.

I would like to thank R. S. Weld, S. Benecchi, and L. Trakimas for expert technical assistance; E. Berthiaume, J. A. Swanson, and K. D. Lee for assistance with ratiometric imaging; S. S. Bowser, J. F. Dice, E. Holtzman, S. Ito, K. S. Matlin, S. L. Palay, and A. Zuk for helpful discussions; and Dr. Stephen Block for the kind gift of computer software.

This work was supported by National Institutes of Health grant NS 27073 and a Basil O'Connor Starter Scholar award from the March of Dimes Birth Defects Foundation.

Received for publication 8 September 1992 and in revised form 4 January 1993.

References

1. Allen, R. D., J. Metuzals, I. Tasaki, S. T. Brady, and S. P. Gilbert. 1982. Fast axonal transport in squid giant axon. *Science (Wash. DC)*. 218: 1127–1129.
2. Allen, R. D., D. G. Weiss, J. H. Hayden, D. T. Brown, H. Fujiwake, and M. Simpson. 1985. Gliding movement of and bidirectional transport along single native microtubules from squid axoplasm: evidence for an active role of microtubules in cytoplasmic transport. *J. Cell Biol.* 100: 1736–1752.

3. Brady, S. T., 1985. A novel brain ATPase with properties expected for the fast axonal transport motor. *Nature (Lond.).* 317:73–75.
4. Brady, S. T., R. J. Lasek, and R. D. Allen. 1982. Fast axonal transport in extruded axoplasm from squid giant axon. *Science (Wash. DC).* 218:1129–1131.
5. Buchner, D., D. Seitz-Tutter, K. Schönitzer, and D. G. Weiss. 1987. A quantitative study of anterograde and retrograde axonal transport of exogenous proteins in olfactory nerve C-fibers. *Neuroscience.* 22:697–707.
6. Bunge, M. B. 1973. Fine structure of nerve fibers and growth cones of isolated sympathetic neurons in culture. *J. Cell Biol.* 56:713–735.
7. Cassel, D., and T. Pfeuffer. 1978. Mechanism of cholera toxin action: covalent modification of the guanyl nucleotide-binding protein of the adenylate cyclase system. *Proc. Natl. Acad. Sci. USA.* 75:2669–2673.
8. Cassel, D., and Z. Selinger. 1977. Mechanism of adenylate cyclase activation by cholera toxin: inhibition of GTP hydrolysis at the regulatory site. *Proc. Natl. Acad. Sci. USA.* 74:3307–3311.
9. Cheng, T. P. O., and T. S. Reese. 1985. Polarized compartmentalization of organelles in growth cones from developing optic tectum. *J. Cell Biol.* 101:1473–1480.
10. Cheng, T. P. O., and T. S. Reese. 1987. Recycling of plasmalemma in chick tectal growth cones. *J. Neurosci.* 7:1752–1759.
11. Clarke, M. S. F., and P. L. McNeil. 1992. Syringe loading introduces macromolecules into living mammalian cytosol. *J. Cell Sci.* 102:533–541.
12. Clement, N. R., and J. M. Gould. 1981. Pyranine (8-hydroxy-1,3,6-pyrenetrisulfonate) as a probe of internal aqueous hydrogen ion concentration in phospholipid vesicles. *Biochemistry.* 20:1534–1538.
13. Croall, D. E., and G. N. DeMartino. 1991. Calcium-activated neutral protease (calpain) system: structure, function, and regulation. *Physiol Rev.* 71:813–847.
14. Dice, J. F., S. R. Terlecky, H.-L. Chiang, T. S. Olson, L. D. Isenman, S. R. Short-Russell, S. Freundlieb, and L. J. Terlecky. 1990. A selective pathway for degradation of cytosolic proteins by lysosomes. *Sem. Cell Biol.* 1:449–455.
15. DiStefano, P. S., B. Friedman, C. Radziejewski, C. Alexander, P. Boland, C. M. Schick, R. M. Lindsay, and S. J. Wiegand. 1992. The neurotrophins BDNF, NT-3, and NGF display distinct patterns of retrograde axonal transport in peripheral and central neurons. *Neuron.* 8:983–993.
16. Dunn, W. A. 1990. Studies on the mechanisms of autophagy: formation of the autophagic vacuole. *J. Cell Biol.* 110:1923–1933.
17. Dunn, W. A. 1990. Studies on the mechanisms of autophagy: maturation of the autophagic vacuole. *J. Cell Biol.* 110:1935–1945.
18. Fabian, R. H. 1991. Retrograde axonal transport and transcytosis of immunoglobulins: implications for the pathogenesis of autoimmune motor neuron disease. *Adv. Neurol.* 56:433–444.
19. Fahim, M. A., R. J. Lasek, S. T. Brady, and A. J. Hodge. 1985. AVEC-DIC and electron microscopic analyses of axonally transported particles in cold-blocked squid giant axons. *J. Neurocytol.* 14:689–704.
20. Finkelstein, R. 1976. Progress in the study of cholera and related toxins. *In* Mechanisms in Bacterial Toxicology. A. Bernheimer, editor. John Wiley Press, NY. 53–84.
21. Furukawa, R., J. E. Wampler, and M. Fechheimer. 1988. Measurement of the cytoplasmic pH of *Dictyostelium discoideum* using a low light level microspectrofluorometer. *J. Cell Biol.* 107:2541–2549.
22. Furukawa, R., J. E. Wampler, and M. Fechheimer. 1990. Cytoplasmic pH of *Dictyostelium discoideum* amebae during early development: identification of two cell subpopulations before the aggregation stage. *J. Cell Biol.* 110:1947–1954.
23. Gill, D., and R. Meren. 1978. ADP-ribosylation of membrane proteins catalyzed by cholera toxin: basis of the activation of adenylate cyclase. *Proc. Natl. Acad. Sci. USA.* 75:3050–3054.
24. Giuliano, K. A., and R. J. Gillies. 1987. Determination of intracellular pH of BALB/c-3T3 cells using the fluorescence of pyranine. *Anal. Biochem.* 167:362–371.
25. Goldberg, A. L. 1992. The mechanism and functions of ATP-dependent proteases in bacterial and animal cells. *Eur. J. Biochem.* 203:9–23.
26. Gordon, P. B., A. L. Kovacs, and P. O. Seglen. 1987. Temperature dependence of protein degradation, autophagic sequestration and mitochondrial sugar uptake in rat hepatocytes. *Biochim. Biophys. Acta.* 929:128–133.
27. Gordon, P. B., and P. O. Seglen. 1988. Prelysosomal convergence of autophagic and endocytic pathways. *Biochem. Biophys. Res. Comm.* 151: 40–47.
28. Gordon, P. B., H. Høyvik, and P. O. Seglen. 1992. Prelysosomal and lysosomal connections between autophagy and endocytosis. *Biochem. J.* 283:361–369.
29. Grafstein, B., and D. S. Forman. 1980. Intracellular transport in neurons. *Physiol. Rev.* 60:1167–1283.
30. Hama, K., and K. Saito. 1977. Fine structure of the afferent synapse of the hair cells in the saccular macula of the goldfish with special reference to the anastomosing tubules. *J. Neurocytol.* 6:361–373.
31. Hendil, K. B. 1981. Autophagy of metabolically inert substances injected into fibroblasts in culture. *Exp. Cell Res.* 135:157–166.
32. Hendry, I. A., K. Stockel, H. Thoenen, and L. L. Iversen. 1974. The retrograde axonal transport of nerve growth factor. *Brain Res.* 68:103–121.
33. Hershko, A. 1991. The ubiquitin pathway for protein degradation. *Trends Biochem. Sci.* 16:265–268.
34. Heuser, J. E., and T. S. Reese. 1973. Evidence for recycling of synaptic vesicle membrane during transmitter release at the frog neuromuscular junction. *J. Cell Biol.* 57:315–344.
35. Hollenbeck, P. J., and D. Bray. 1987. Rapidly transported organelles containing membrane and cytoskeletal components: their relation to axonal growth. *J. Cell Biol.* 105:2827–2835.
36. Holtzman, E. 1971. Cytochemical studies of protein transport in the nervous system. *Philos. Trans. R. Soc. Lond. B. Biol. Sci.* 261:407–421.
37. Holtzman, E. 1989. Autophagy and related phenomena. *In* Lysosomes. Plenum Press, NY. 243–317.
38. Høyvik, H., P. B. Gordon, T. O. Berg, P. E. Stromhaug, and P. O. Seglen. 1991. Inhibition of autophagic-lysosomal delivery and autophagic lactolysis by asparagine. *J. Cell Biol.* 113:1305–1312.
39. Kano, K., and J. H. Fendler. 1978. Pyranine as a sensitive pH probe for liposome interiors and surfaces. pH gradients across phospholipid vesicles. *Biochem. Biophys. Acta.* 509:289–299.
40. Koptiz, J., G. O. Kisen, P. B. Gordon, P. Bohley, and P. O. Seglen. 1990. Nonselective autophagy of cytosolic enzymes by isolated rat hepatocytes. *J. Cell Biol.* 111:941–953.
41. Kovács, A. L., B. Grinde, and P. O. Seglen. 1981. Inhibition of autophagic vacuole formation and protein degradation by amino acids in isolated hepatocytes. *Exp. Cell Res.* 133:431–436.
42. Kovács, A. L., A. Reith, and P. O. Seglen. 1982. Accumulation of autophagosomes after inhibition of hepatocytic protein degradation by vinblastine, leupeptin or a lysosomotropic amine. *Exp. Cell Res.* 137: 191–201.
43. Kristensson, K. 1978. Retrograde transport of macromolecules in axons. *Annu. Rev. Pharmacol. Toxicol.* 18:97–110.
44. Lander, A. D., D. K. Fujii, D. Gospodarowicz, and L. F. Reichardt. 1982. Characterization of a factor that promotes neurite outgrowth: evidence linking activity to a heparan sulfate proteoglycan. *J. Cell Biol.* 94:574–585.
45. Lee, H. C. 1985. The voltage-sensitive Na+/H+ exchange in sea urchin spermatozoa flagellar membrane vesicles studied with an entrapped pH probe. *J. Biol. Chem.* 260:10794–10799.
46. Liscum, L., P. J. Hauptman, D. C. Hood, and E. Holtzman. 1982. Effects of barium and tetramethylammonium on membrane circulation in frog retinal photoreceptors. *J. Cell Biol.* 95:296–309.
47. Margiotta, J., D. Berg, and V. Dionne. 1987. Cyclic AMP regulates the proportion of functional acetylcholine receptors on chicken ciliary ganglion neurons. *Proc. Natl. Acad. Sci. USA.* 84:8155–8159.
48. Martinez, R., R. J. Gillies, and K. A. Giuliano. 1988. Effect of serum on the intracellular pH of BALB/c-3T3 cells: serum deprivation causes changes in sensitivity of cells to serum. *J. Cell. Physiol.* 136:154–160.
49. Mortimore, G. E. 1987. Mechanism and regulation of induced and basal protein degradation in liver. *In* Lysosomes: Their Role in Protein Breakdown. H. Glaumann and F. J. Ballard, editors. Academic Press, London. 415–443.
50. Mortimore, G. E,. and W. F. Ward. 1981. Internalization of cytoplasmic protein by hepatic lysosomes in basal and deprivation-induced proteolytic states. *J. Biol. Chem.* 256:7659–7665.
51. Parton, R. G., K. Simons, and C. G. Dotti. 1992. Axonal and dendritic pathways in cultured neurons. *J. Cell Biol.* 119:123–137.
52. Paschal, B. M., and R. B. Vallee. 1987. Retrograde transport by the microtubule-associated protein MAP 1C. *Nature (Lond.).* 330:181–183.
53. Peters, A., S. L. Palay, and H. D. Webster. 1976. The Fine Structure of the Nervous System: The Neurons and Supporting Cells. W.B. Saunders Co., Philadelphia. 1–406.
54. Plomp, P. J., P.B. Gordon, A. J. Meijer, H. Høyvik, and P. O. Seglen. 1989. Energy dependence of different steps in the autophagic-lysosomal pathway. *J. Biol. Chem.* 264:6699–6704.
55. Pontremoli, S., and E. Melloni. 1986. Extralysosomal protein degradation. *Annu. Rev. Biochem.* 55:455–481.
56. Punnonen, E. L., and H. Reunanen. 1990. Effects of vinblastine, leucine, and histidine, and 3-methyladenine on autophagy in Ehrlich ascites cells. *Exp. Mol. Pathol.* 52:87–97.
57. Reunanen, H., M. Marttinen, and P. Hirsimaki. 1988. Effects of griseofulvin and nocodazole on the accumulation of autophagic vacuoles in Ehrlich ascites tumor cells. *Exp. Mol. Pathol.* 48:97–102.
58. Russell, L. D., N. K . Saxena, and T. T. Turner. 1989. Cytoskeletal involvement in spermiation and sperm transport. *Tissue & Cell.* 21:361–379.
59. Schaeffer, S. F., and E. Raviola. 1978. Membrane recycling in the cone cell endings of the turtle retina. *J. Cell Biol.* 79:802–825.
60. Schnapp, B. J., and T. S. Reese. 1989. Dynein is the motor for retrograde axonal transport of organelles. *Proc. Natl. Acad. Sci. USA.* 86:1548–1552.
61. Schnapp, B. J., R. D. Vale, M. P. Sheetz, and T. S. Reese. 1985. Single microtubules from squid axoplasm support bidirectional movement of organelles. *Cell.* 40:455–462.
62. Schwartz, J. H. 1979. Axonal transport: components, mechanisms, and specificity. *Annu. Rev. Neurosci.* 2:467–504.
63. Schworer, C. M., K. A. Shiffer, and G. E. Mortimore. 1981. Quantitative relationship between autophagy and proteolysis during graded amino acid deprivation in perfused liver. *J. Biol. Chem.* 256:7652–7658.

64. Seamon, K. B., and J. W. Daly. 1983. Forskolin, cyclic AMP and cellular physiology. *Trends Pharmacol. Sci.* 4:120–123.
65. Seamon, K. B., W. Padgett, and J. W. Daly. 1981. Forskolin: unique diterpene activator of adenylate cyclase in membranes and intact cells. *Proc. Natl. Acad. Sci. USA.* 78:3363–3367.
66. Seglen, P. O. 1987. Regulation of autophagic liver protein degradation in isolated liver cells. *In* Lysosomes: Their Role in Protein Breakdown. Academic Press, London. 371–414.
67. Seglen, P. O., and P. B. Gordon. 1984. Amino acid control of autophagic sequestration and protein degradation in isolated rat hepatocytes. *J. Cell Biol.* 99:435–444.
68. Seglen, P. O., P. B. Gordon, H. Tolleschaug, and H. Høyvik. 1985. Pathways of intracellular sequestration and protein degradation in isolated rat hepatocytes. *In* Intracellular Protein Catabolism, E. A. Khairallah, J. S. Bond, and J. W. C. Bird, editors. Alan R. Liss, NY. 437–446.
69. Seglen, P. O., P. B. Gordon, and I. Holen. 1990. Non-selective autophagy. *Sem. Cell Biol.* 1:441–448.
70. Smith, R. S. 1980. The short term accumulation of axonally transported organelles in the region of localized lesions of single myelinated axons. *J. Neurocytol.* 9:39–65.
71. Stacey, D. W., and V. G. Allfrey. 1977. Evidence for the autophagy of microinjected proteins in HeLa cells. *J. Cell Biol.* 75:807–817.
72. Steinberg, T. H., J. A. Swanson, and S. C. Silverstein. 1988. A prelysosomal compartment sequesters membrane-impermeant fluorescent dyes from the cytoplasmic matrix of J774 macrophages. *J. Cell Biol.* 107:887–896.
73. Toyoshima, I., H. Yu, E. R. Steuer, and M. P. Sheetz. 1992. Kinectin, a major kinesin-binding protein on ER. *J. Cell Biol.* 118:1121–1131.
74. Tsukita, S., and H. Ishikawa. 1980. The movement of membranous organelles in axons. *J. Cell Biol.* 84:513–530.
75. Vale, R. D., T. S. Reese, and M. P. Sheetz. 1985. Identification of a novel force-generating protein, kinesin, involved in microtubule-base motility. *Cell.* 42:39–50.
76. Vale, R. D., B. J. Schnapp, T. Mitchison, E. Steuer, T. S. Reese, and M. P. Sheetz. 1985. Different axoplasmic proteins generate movement in opposite directions along microtubules in vitro. *Cell.* 43:623–632.
77. Vallee, R. B., and H. S. Shpetner. 1990. Motor proteins of cytoplasmic microtubules. *Annu. Rev. Biochem.* 59:909–932.
78. Weiss, D. G., G. M. Langford, D. Seitz-Tutter, and F. Keller. 1988. Dynamic instability and motile events of native microtubules from squid axoplasm. *Cell Motil. Cytoskeleton.* 10:285–295.
79. Wolfbeis, O. S., E. Furlinger, H. Kroneis, and H. Marsoner. 1983. A study on fluorescent indicators for measuring near neutral ("physiological") pH-values. *Fresenius Z. Anal. Chem.* 314:119–124.